CHEMISTRY
A EUROPEAN JOURNAL

Supporting Information

Self-Organizing Domino-Like Superlattices through Stereochemical Recognition Match at the Organic–Inorganic Interface in Solution

An-Xiang Yin, Ya-Wen Zhang,* and Chun-Hua Yan*[a]

chem_201101005_sm_miscellaneous_information.pdf

Experimentation

A Schlenk line system was employed in the nanocrystal synthesis. Oleic acid (OA; 90%, Aldrich), oleylamine (OM; > 80%, Acros), hexadecylamine (HDA; > 90%, Acros), octadecylamine (ODA; > 90%, Acros), stearic acid (AR, Beijing Chemical Reagents Company), lauric acid (AR, Beijing Chemical Reagents Company), trifluoroacetic acid (99%, Acros), trichloroacetic acid (99%, Acros), tribromoacetic acid (99%, Aldrich), absolute ethanol, cyclohexane and toluene were used as received.

Preparation of $M(CX_3COO)_2$ (M = Ba, Sr, Ca; X = F, Cl, Br) precursors. $M(CX_3COO)_2$ (M = Ba, Sr, Ca; X = F, Cl, Br) salts were prepared by mixing MCO_3 (M = Ba, Sr, Ca) with ~ 10% excess aqueous solution of CX_3COOH (X = F, Cl, Br) with gentle stirring at room temperature. The result transparent solution was boiled to evaporate the excess acids, and then evaporated and dried in an oven at 140 ℃ for 24 h (For $Ca(CCl_3COO)_2$ and $Ba(CBr_3COO)_2$ a lower temperature of 120 ℃ was used). The remaining white powders were collected for further reactions and TG-DTA analysis.

Syntheses of BaFCl, SrFCl, BaFBr, and CaFCl nanocrystals. In a typical synthesis route, 0.5 mmol of $Ba(CF_3COO)_2$ and 0.5 mmol of $Ba(CCl_3COO)_2$ were mixed with the solution of OA (4 mmol) and OM (36 mmol) in a three-necked flask at room temperature, and then degassed and heated to 140 ℃ with vigorous magnetic stirring for 15 min to remove water and other impurities with low boiling points. Next, the colorless, transparent solution was heated to 300 ℃ at a heating rate of 20 ℃·min^{-1} under a high purified N_2 atmosphere. After 30 minutes of reaction, the white turbid solution was left to be cooled to room temperature by air with gentle stirring for 5-10 min. Then the white gel-like product was separated by centrifuging and washed several times with cyclohexane and ethanol, and followed by drying at 80 ℃ for 12 h, showing a yield of ca. 80%. The as-dried product is dispersible in nonpolar solvents such as cyclohexane and toluene.

SrFCl, BaFBr and CaFCl nanocrystals were prepared with the same procedure used for BaFCl nanoplates, except that using different $M(CX_3COO)_2$ precursors, respectively.

Synthesis of BaFCl powders. Un-doped BaFCl powders were prepared through a modified route described in Ref. S1.

Synthesis of Pr_2O_3 nanodisks. Pr_2O_3 nanodisks were obtained through the same procedure described in Ref. S2, except that using the precursor of $Pr(acac)_3{\bullet}2H_2O$ instead of $Pr(BA)_3{\bullet}2H_2O$.

Instrumentation

XRD. Wide Angle X-ray diffraction (WAXRD) patterns of the dry powders were recorded on a Rigaku D/MAX-2000 diffractometer (Japan) with a slit of 1/2 °at a scanning rate of 4 °min^{-1} using Cu K_α radiation (λ = 1.5406 Å). Small Angle XRD (SAXRD) measurements were performed on the same instrument with a slit of 1/6 °at a scanning rate of 1 °min^{-1}.

TEM, HRTEM & EDS. Samples for transmission electron microscopy (TEM) analysis were prepared by drying a drop of diluted colloid solution of BaFCl nanocrystals in cyclohexane on copper grids coated by amorphous carbon. Particle sizes and shapes were examined by a TEM (JEM-2100, JEOL, Japan) operated at 200 kV. High resolution TEM (HRTEM) and energy dispersive X-ray spectroscopy (EDS) analysis was performed on a FEG-TEM (JEM-2100F, JEOL, Japan) operated at 200 kV.

FTIR. FTIR analyses of the the as-prepared samples and surfactant solutions were

performed on a Bruker Vector22 FTIR spectrometer.

TG-DTA. TG-DTA analyses of the $Ba(CX_3COO)_2$ (X = F, Cl) salts were performed on a Q600 SDT Simultaneous DSC-TGA heat flow analyzer (Thermal Analysis, USA) under N_2 or air atmospheres. The samples were heated from RT to 400 ℃ at a heating rate of 10 ℃ min^{-1}.

DLS. The DLS size distribution characterizations of the as-prepared organic-inorganic superlattice dispersions in cyclohexane were performed on a Horiba SZ-100 nano-particle analyzer (Horiba, Japan).

Photoluminescence. The UV-simulated photoluminescence properties of as-prepared BaFCl superstructures at RT were measured on a Hitachi F-4500 fluorescence spectrophotometer (Japan) with a Xenon lamp as a stimulation source. The scanning speed was fixed at 60 nm min^{-1} with both the excitation and emission splits fixed at 2.5 nm.

Supplementary Data

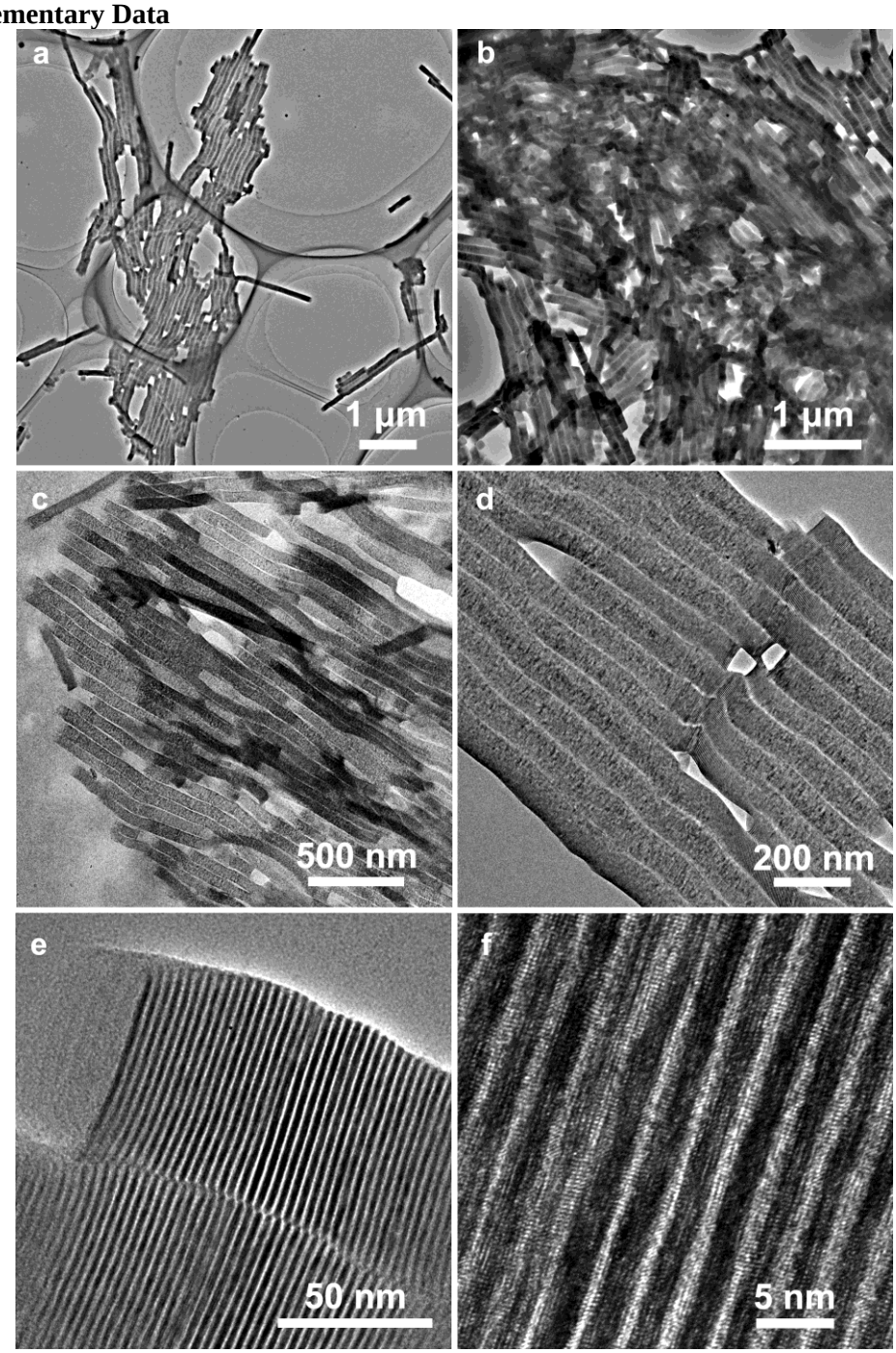

Figure S1. (a-e) TEM & (f) HRTEM images of the superstructures of the self-assembled ultrathin BaFCl nanoplates prepared in the mixed solution of OA (4 mmol) and OM (36 mmol).

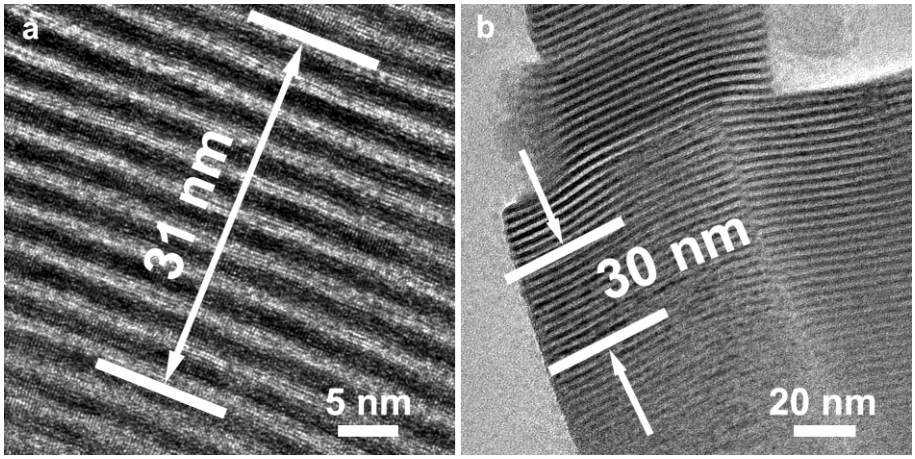

Figure S2. TEM images of the 1D superstructure of the BaFCl nanoplates, showing the thickness of the nanoplates and the interplate distance. The labels are the thickness of 10 layers of the repeating units of the ultrathin nanoplates and the surfactant layers.

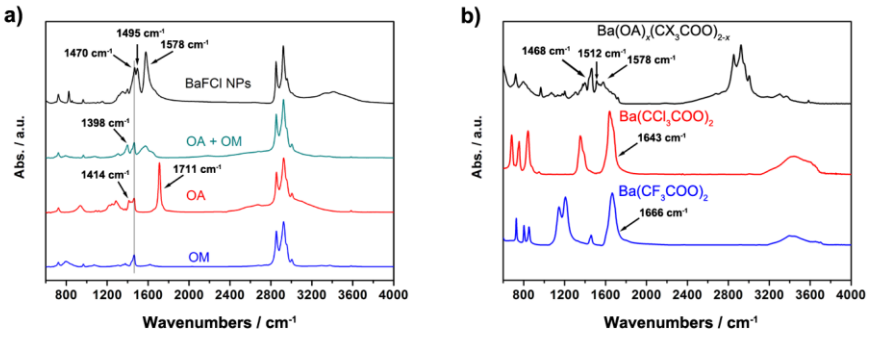

Figure S3. (a) FTIR spectra of the BaFCl nanoplates, mixture of OA and OM (OA : OM = 4 : 36), sole OA, and sole OM. (b) FTIR spectra of the $Ba(OA)_x(CX_3COO)_{2-x}$ complexes, $Ba(CCl_3COO)_2$ powder, and $Ba(CF_3COO)_2$ powder. The shift of the ν_{CO} vibrations between free OA molecules and the washed BaFCl nanoplates (from 1711 cm^{-1} to 1578 cm^{-1}) confirmed the formation of coordination bonds between carboxylic groups of OA molecules with cations on the surfaces of the BaFCl nanoplates (panel a). The formation of $Ba(OA)_x(CX_3COO)_{2-x}$ complexes during the thermal treatment of $Ba(CX_3COO)_2$ precursors in the mixed solution of OA and OM ($Ba(CF_3COO)_2$: $Ba(CF_3COO)_2$: OA : OM = 0.5 mmol : 0.5 mmol : 4 mmol : 36 mmol, 140 ℃, degassed, 15 min) was also confirmed by the significant shift of the ν_{CO} vibrations (from 1666 cm^{-1} and 1643 cm^{-1} to 1578 cm^{-1}), as shown in panel b (Ref. S3-5).

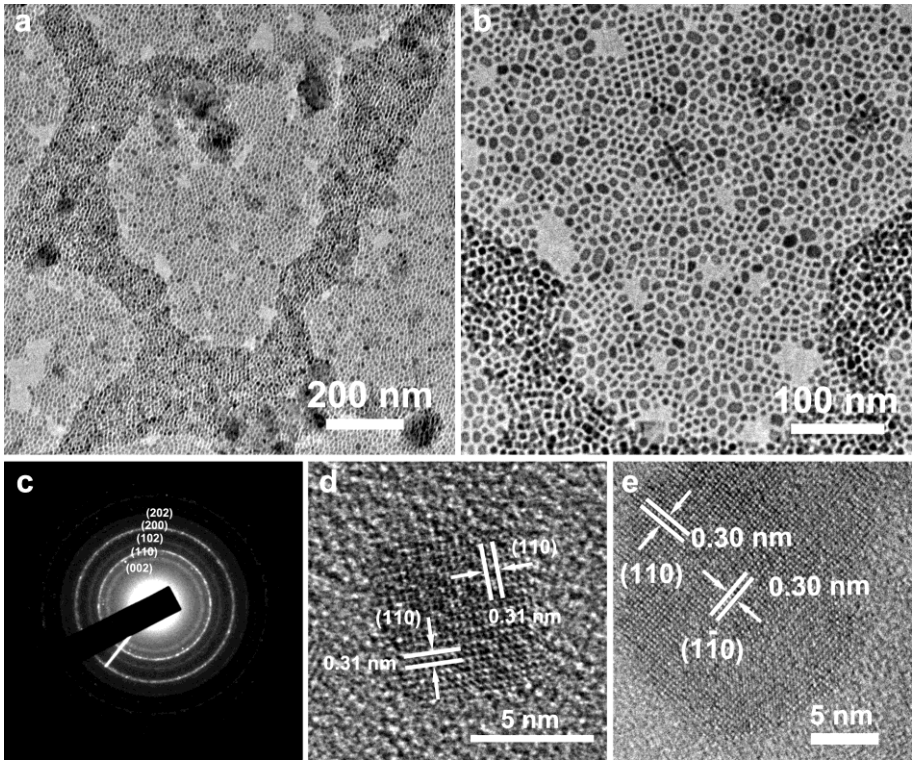

Figure S4. TEM, SAED and HRTEM characterizations of the BaFCl nanocrystals prepared in neat OM (1 mmol of Ba^{2+} in 40 mmol of OM) at 300 ℃ for 30 min: (a – b) TEM images of the BaFCl nanocrystals; (c) SAED pattern of the BaFCl nanocrystals in panel b; (d – e) HRTEM images of two distinct nanocrystals shown in panel b.

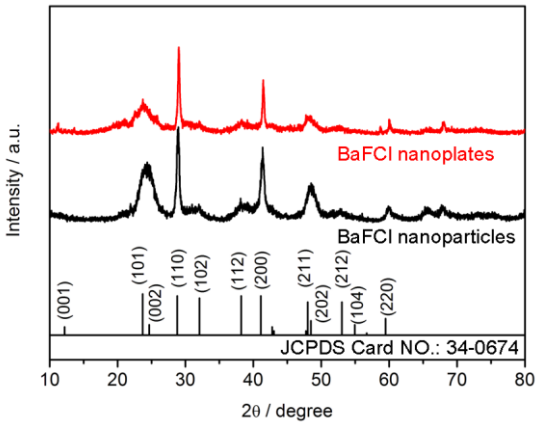

Figure S5. WAXRD patterns of the BaFCl nanoplates and nanocrystals prepared in OA/OM or neat OM, respectively.

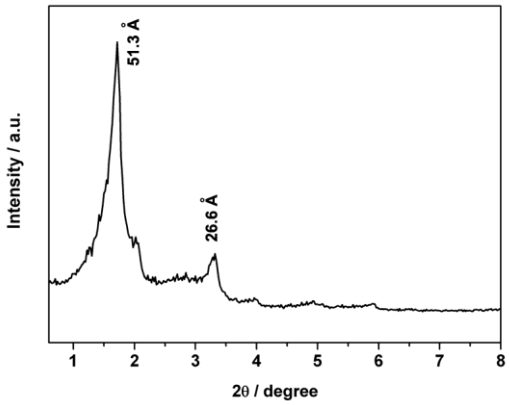

Figure S6. SAXRD pattern of the dried powders of the ultrathin BaFCl nanoplates after being washed with cyclohexane and ethanol several times and then dried at 80 ℃ for 12 h.

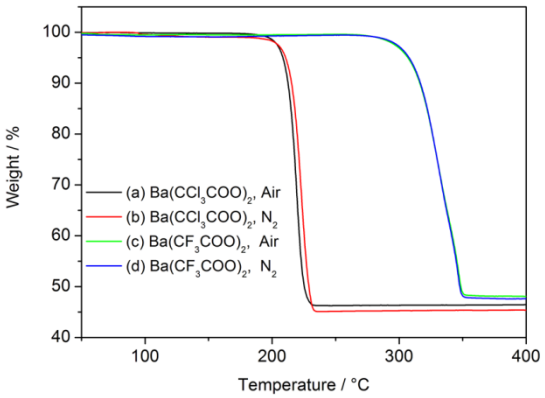

Figure S7. TG curves of $Ba(CX_3COO)_2$ (X = F, Cl) powders heated in different atmospheres: (a) and (c) in air; (b) and (d) in N_2.

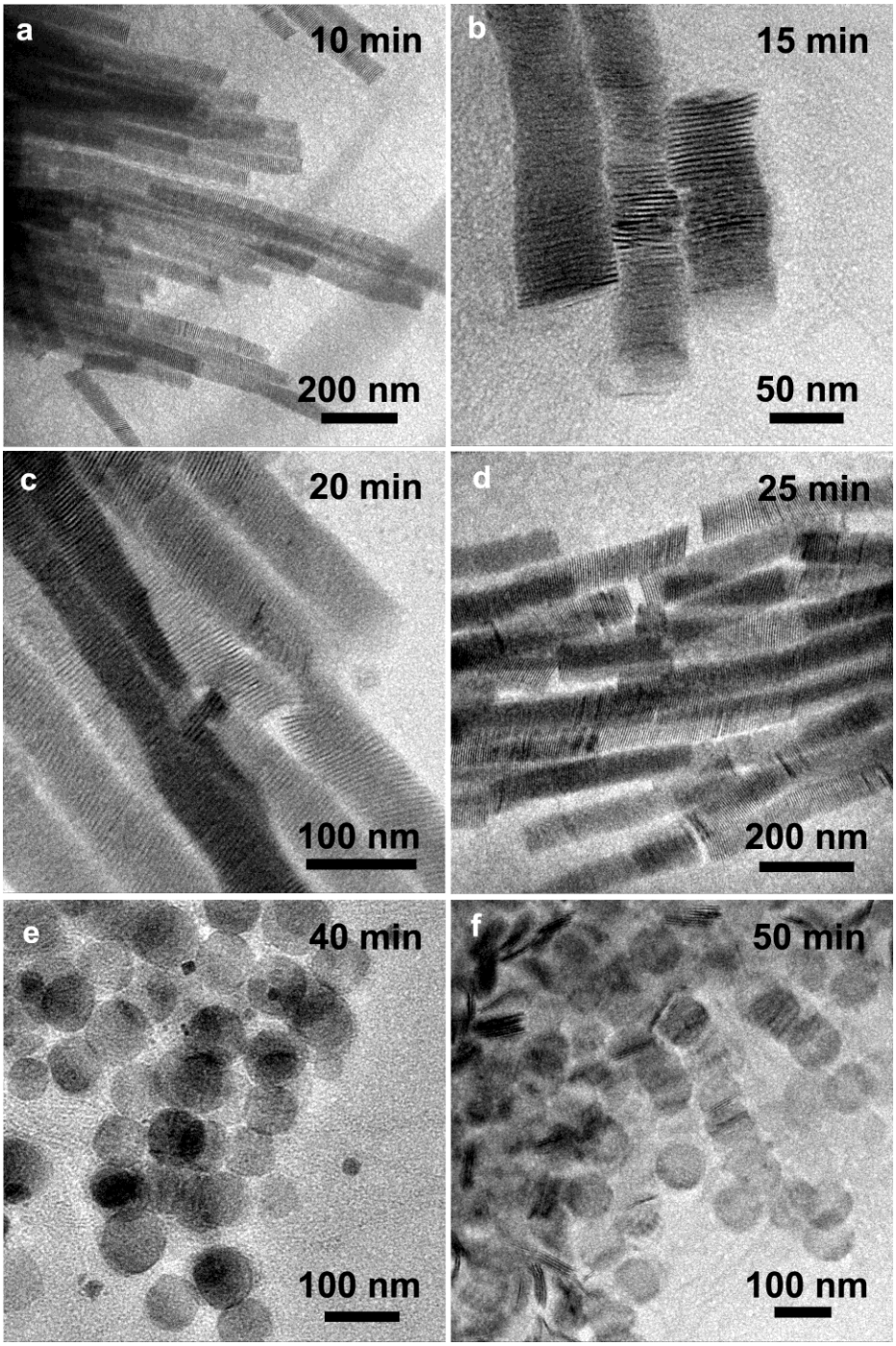

Figure S8. Temporal size and shape evolution of the as-prepared BaFCl nanocrystals: (a) 10 min; (b) 15 min; (c) 20 min; (d) 25 min; (e) 40 min; (f) 50 min.

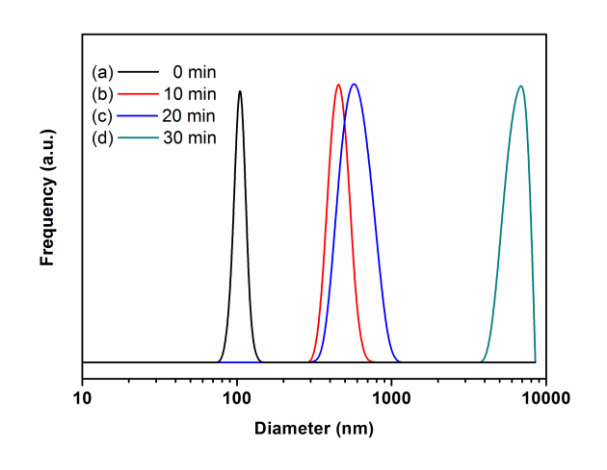

Figure S9. DLS curves of the size distributions of the as-prepared BaFCl-based organic-inorganic superstructures in reaction solution at: (a) 0 min, (b) 10 min, (c) 20 min and (d) 30 min. DLS signals of the above samples (b), (c) and (d) filtrated with a 0.22 μm filter and the precursor solution ($Ba(CF_3COO)_2$: $Ba(CF_3COO)_2$: OA : OM = 0.5 : 0.5 : 4 : 36) were very weak and no distribution curves could be obtained, indicating that few small nanoparticles could be detected by the DLS analyzer in these clean solutions.

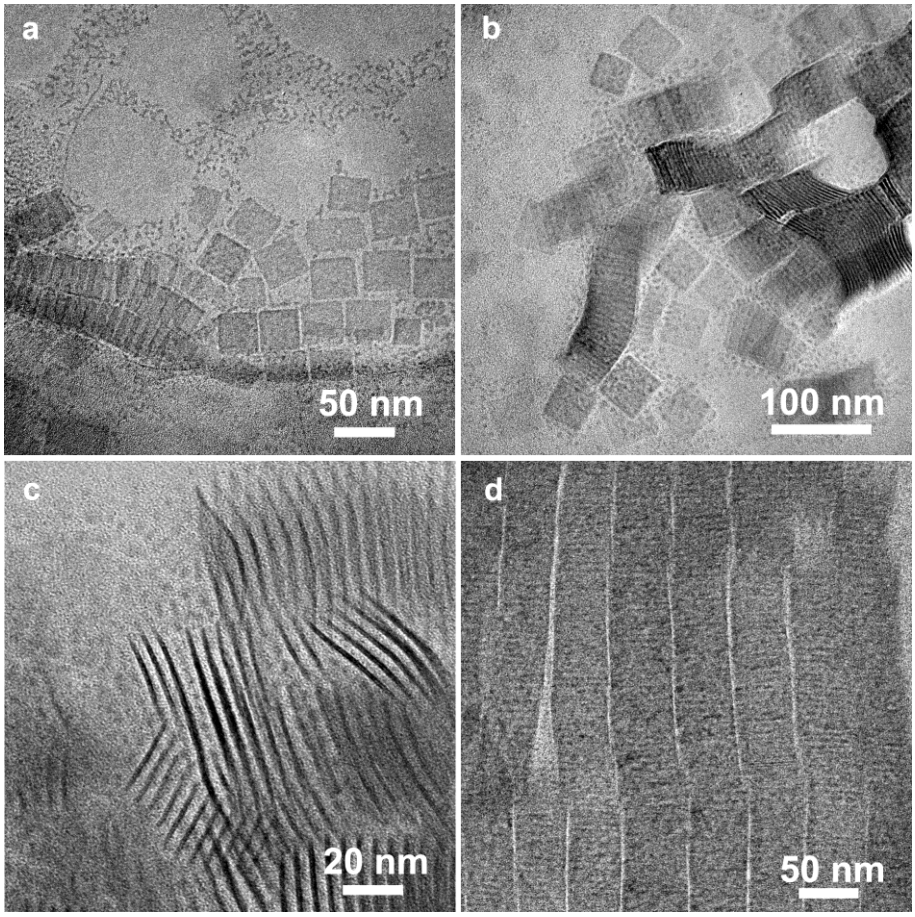

Figure S10. TEM images illustrating the disassembly behavior of the 1D superstructures of the ultrathin BaFCl nanoplates: (a) disassembled BaFCl nanoplates after refluxing for 3 h in toluene; (b) disassembled BaFCl nanoplates after sonication for 1 h in toluene; (c) disassembled single-layered thin BaFCl nanoplates after sonication for 1 h in toluene; (d) unaltered BaFCl superstructures after refluxing in cyclohexane for 3 h.

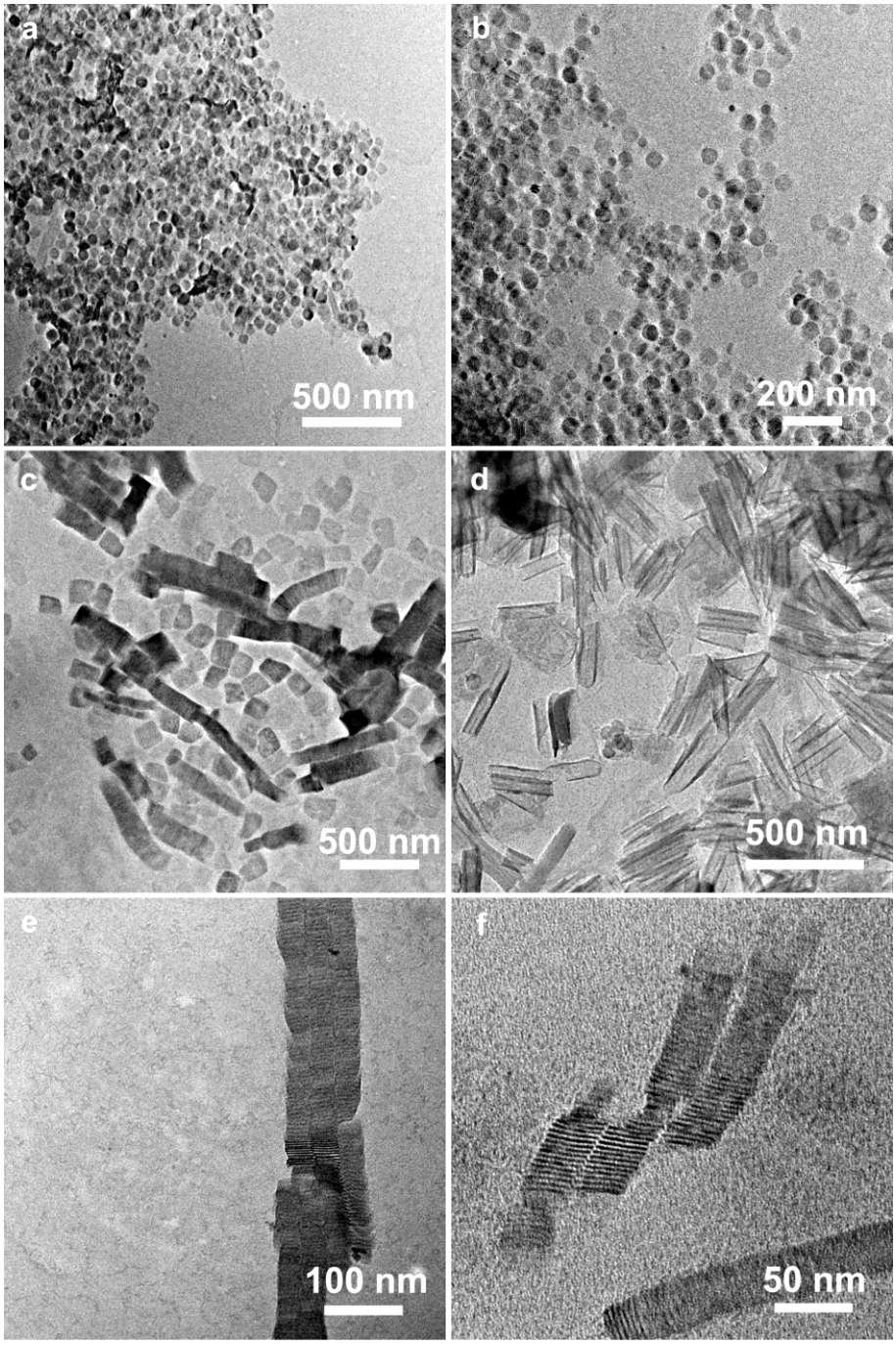

Figure S11. TEM images of BaFCl nanocrystals prepared in different surfactant solutions with the same precursor concentrations at 300 ℃ for 30 min: (a) OA : SA : OM = 3 : 1 : 36; (b) SA : OM = 4 : 36; (c) OA : LA : OM = 3 : 1 : 36; (d) LA : OM = 4 : 36; (e) SA : ODA = 4 : 36; (f) SA : HDA = 4 : 36.

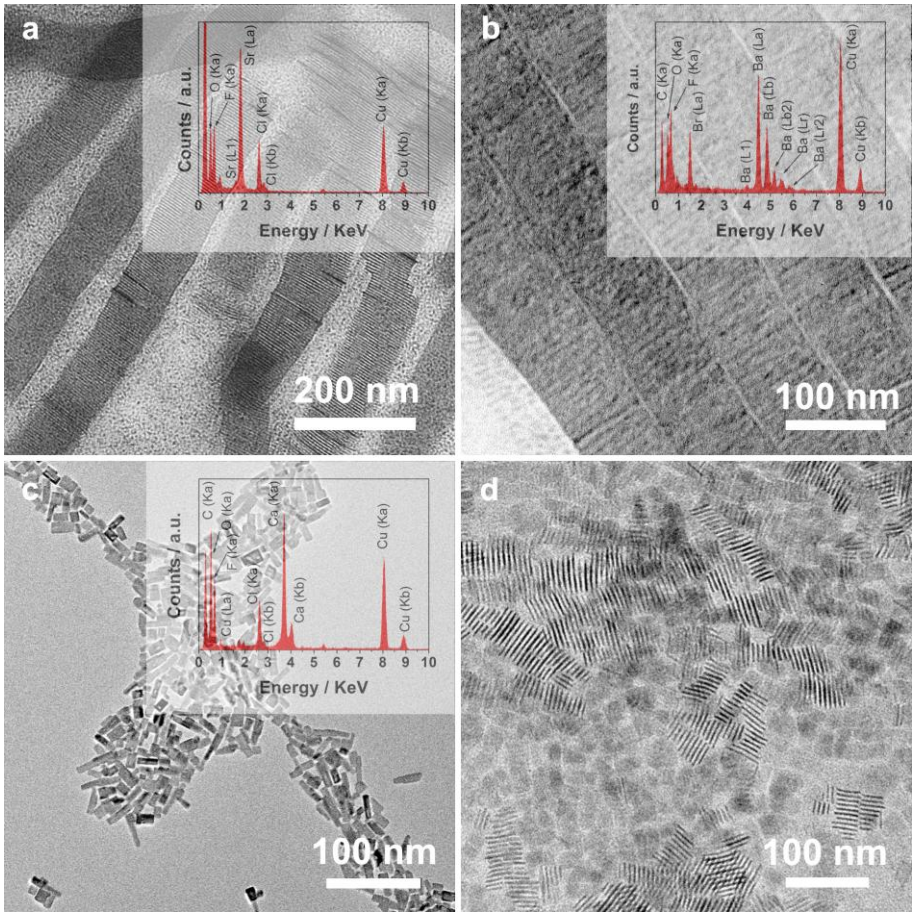

Figure S12. TEM images of (a) SrFCl, (b) BaFBr, (c) CaFCl and (d) Pr_2O_3 nanocrystals prepared under the similar conditions with the BaFCl nanoplates, where M : OA : OM = 1 : 4 : 36 (M = Sr, Ba, Ca, Pr). Insets in panel a, b, and c show the EDS results of SrFCl, BaFBr, and CaFCl nanoplates, respectively (Sr : F : Cl : O = 39.6 : 29.2 : 11.6 : 25.4 for SrFCl; Ba : F : Br : O = 35.6 : 26.0 : 17.2 : 21.2 for BaFBr; Ca : F : Cl : O = 15.6 : 16.7 : 9.8 : 35.8 for CaFCl).

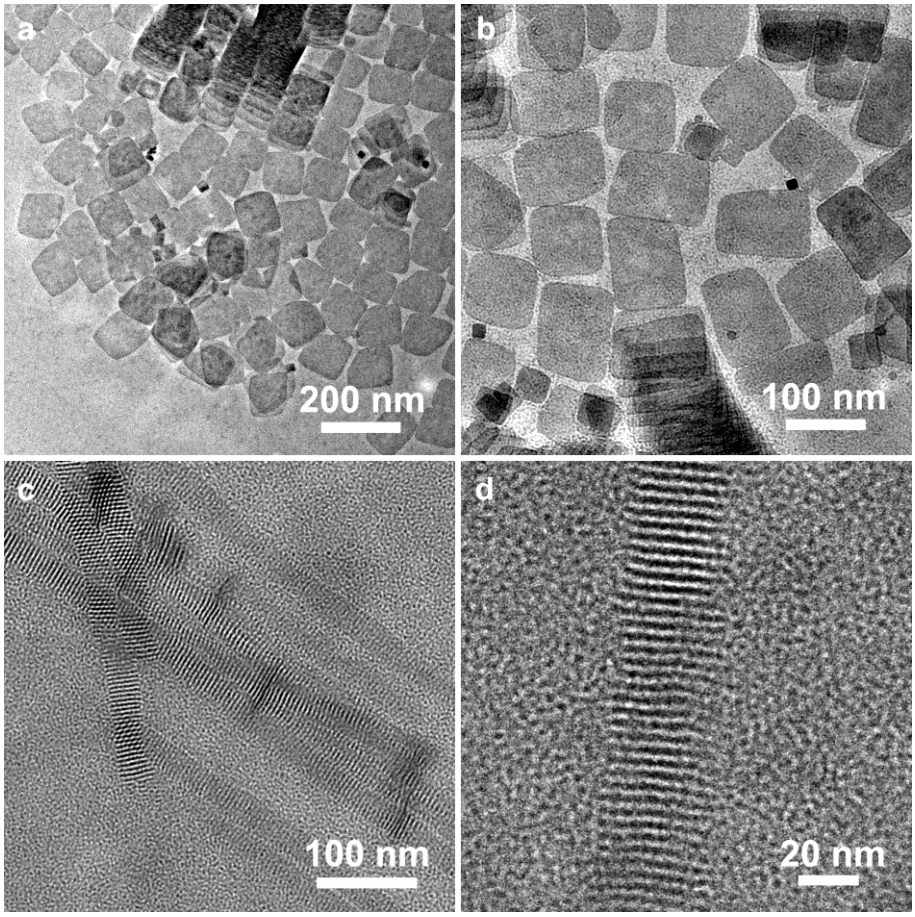

Figure S13. TEM images of BaFCl nanoplates prepared with different initial Ba^{2+} concentrations at 300 ℃ for 30 min: (a) and (b) Ba^{2+} : OA : OM = 0.5 mmol : 4 mmol : 36 mmol; (c) and (d) Ba^{2+} : OA : OM = 2 mmol : 4 mmol : 36 mmol.

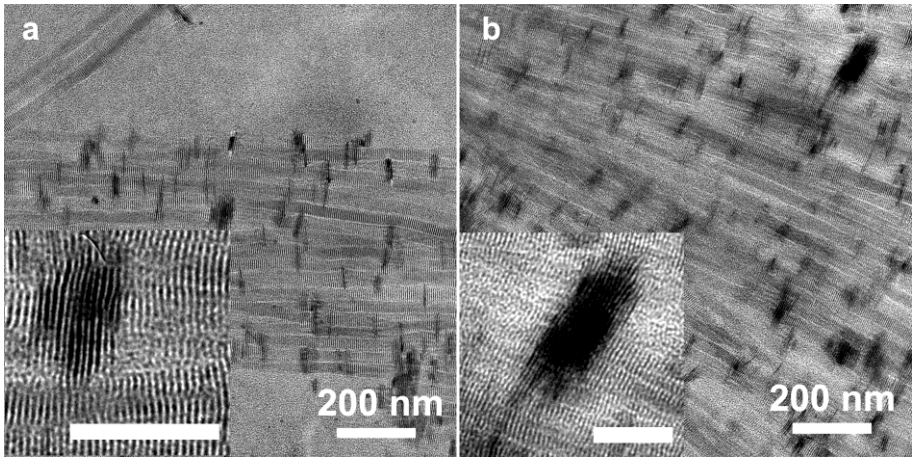

Figure S14. TEM images of 1D assembly of ultrathin BaFCl nanoplates (Ba^{2+} : OA : OM = 2 : 4 : 36), showing the distortions of the micelle structure and the formation of some large nanoplates growing across several nearby micelle chains. The insets are magnifications of typical areas of each panel. The length of the scale bar in each inset is 100 nm.

Modeling of the surface adsorption & self-assembly features of the BaFCl nanoplates

In the modeling, the oxygen atoms of the OA molecules were assumed to replace the surface halide species (esp. Cl^-) to coordinate with the surface Ba^{2+} cations, as indicated by the EDS results.

As shown in Figure S15, the BaFCl crystal is of the matlockite tetragonal structure (Space group: *P4/nmm*) with the lattice parameters of $a = b = 4.396$ Å, $c = 7.231$ Å and $\alpha = \beta = \gamma = 90$ °. The distribution of Cl^- and F^- anions on the facets of (001), (100) and (110) of a perfect BaFCl crystal was shown in Figure S16. The distances of nearby halide anions in the same layer of a specific facet are listed in Table S1.

A brief MM calculation revealed that the distance between the two oxygen atoms in a OA molecule were approximately 2.34 Å, suggesting that the two oxygen atoms of a single OA molecule can only replace one Cl^- (F^-) anions instead of two nearby halide anions in the same layer of the (001), (110) and (100) facets of BaFCl nanocrystals because the distances between any nearby two anions on the same facet of the BaFCl crystal are much longer than the calculated 2.34 Å. Thus, we assume that one surfactant molecule can only replace one halide anions (esp. Cl^-) on the surface of BaFCl nanocrystals.

Moreover, as shown in Figure S16 and Table S1, the densities of halide anions on different facets of a BaFCl crystal follow the discipline of (100) < (001) < (110) for Cl^- and (100) < (110) < (001) for F^-. Hence, the adsorption of OA molecules, i.e. the replacement of surface Cl^- by OA, on the (001) and (110) facets would be more favorable in energy. Thus, the selective adsorption of surfactants, as well as the soft-template effects of the micelles, leading to the faster growth of the nanocrystal on the (100) facets and the formation of the ultrathin BaFCl nanoplates of rectangle shapes (Figure S17) instead of the small nanoparticles with irregular shapes prepared in sole OM (Figure S4).

The model of the self-assembled layered nanoplates with interplate penetrated single layer of surfactants (Figure 4) was established based on the TEM observations and SAXRD analyses, as well as several model studies of the surface adsorbed surfactant layers on solid facets (Ref. S6). The steric energy of the carbon chains was then calculated and optimized with the MMX force field. With the end of each OA (SA) molecule fixed at the tetrahedral lattice, rotation, tilting and bending of the carbon chains are allowed in the computations.

Table S1. Distances of two closest nearby halide anions in the same facets of BaFCl crystals.

Facets	Cl^-		F^-	
	a^* (Å)	b^*(Å)	a^*(Å)	b^*(Å)
(001)	4.396	4.396	3.108	3.108
(100)	4.396	7.231	4.396	7.231
(110)	3.797	3.797	3.108	7.231

* a and b represent two directions of the closest two Cl^- (F^-) anions on the same facets

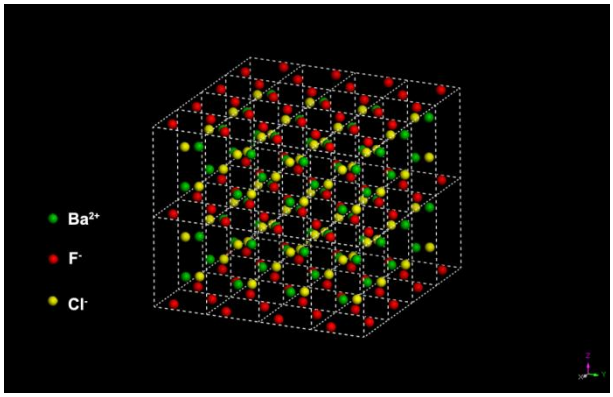

Figure S15. Crystal structure of BaFCl (Matlockite structure, Tetragonal, *P4/nmm*).

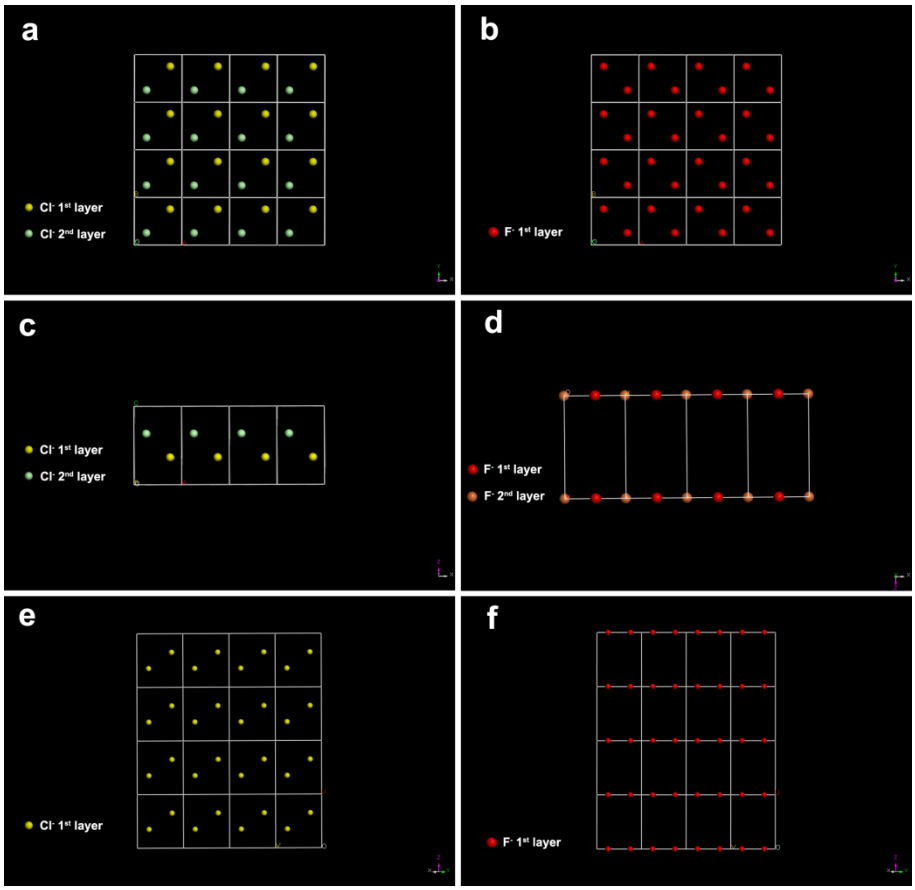

Figure S16. Distributions of Cl^- and F^- on different facets of BaFCl crystal: (a) Cl^- and (b) F^- on the (001) facet; (c) Cl^- and (d) F^- on the (100) facet; (e) Cl^- and (f) F^- on the (110) facet.

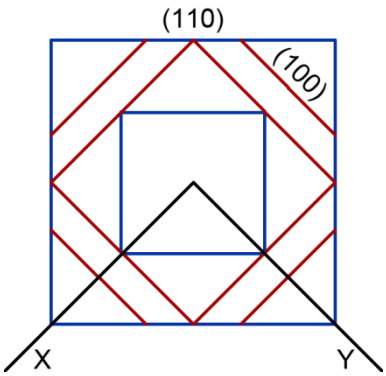

Figure S17. Illustration for the formation procedure of the rectangle shaped nanoplates bounded by (110) facets. The growth rate of the (100) facets (red line) is faster than the one of the (110) facets (blue line) and thus lead to the rectangle shaped nanoplates bounded by (110) facets.

References

[S1] Ju, Q., Liu, Y. S., Li, R. F., Liu, L. Q., Luo, W. Q., Chen, X. Y. *J. Phys. Chem. C* **2009,** *113*, 2309-2315.

[S2] Si, R., Zhang, Y. W., You, L. P., Yan, C. H. *Angew. Chem. Int. Ed.* **2005**, *44***,** 3256-3260.

[S3] Herranz, F., Morales, M. P., Roca, A. G., Desco, M., Ruiz-Cabello, J. *Chem. Eur. J.* **2008**, *14*, 9126-9130.

[S4] Chen, Z. G., Chen, H. L., Hu, H., Yu, M. X., Li, F. Y., Zhang, Q., Zhou, Z. G., Yi, T., Huang, C. H. *J. Am. Chem. Soc.* **2008**, *130*, 3023-3029.

[S5] Du, Y. P., Zhang, Y. W., Yan, Z. G., Sun, L. D., Gao, S., Yan, C. H. *Chem. Asian J.* **2007**, *2*, 965-974.

[S6] Ulman, A. *Chem. Rev.* **1996,** *96*, 1533-1554.